World Academy of Science, Engineering and Technology
International Journal of Mechanical and Mechatronics Engineering
Vol:15, No:11, 2021

Simulation with Uncertainties of Active Controlled Vibration Isolation System for Astronaut's Exercise Platform

Shield B. Lin, Ziraguen O. Williams

***Abstract*—**In a task to assist NASA in analyzing the dynamic forces caused by operational countermeasures of an astronaut's exercise platform impacting the spacecraft, an active proportional-integral-derivative controller commanding a linear actuator is proposed in a vibration isolation system to regulate the movement of the exercise platform. Computer simulation shows promising results that most exciter forces can be reduced or even eliminated. This paper emphasizes on parameter uncertainties, variations and exciter force variations. Drift and variations of system parameters in the vibration isolation system for astronaut's exercise platform are analyzed. An active controlled scheme is applied with the goals to reduce the platform displacement and to minimize the force being transmitted to the spacecraft structure. The controller must be robust enough to accommodate the wide variations of system parameters and exciter forces. Computer simulation for the vibration isolation system was performed via MATLAB/Simulink and Trick. The simulation results demonstrate the achievement of force reduction with small platform displacement under wide ranges of variations in system parameters.

***Keywords*—**Control, counterweight, isolation, vibration.

I. Introduction

IT is extremely important for astronauts to have sufficient exercise during space missions [1], [2]. Without a special isolation device, exercise activities inevitably produce excited forces that are transmitted to the spacecraft and may cause operation difficulty. In an effort to minimize the transmitted forces, the use of vibration isolation systems (VIS) has been studied in a microgravity environment [3], [4].

Proportional-integral-derivative (PID) controllers have been used to direct the motion control in various applications [5]-[8]. A one-dimensional (1D) active controlled VIS was developed and published by [9]. As shown in Fig. 1 [9], a Simulink diagram of a 1D VIS for astronaut's exercise platform uses a discrete PID controller to command a DC motor and a lead screw to push and pull a counterweight which injects actuator force to the system. The platform displacement is the primary controlled variable with the goal to minimize its movement around the initial location. The PID control algorithms calculate a voltage command to drive a DC motor with inductance, L_a, resistance, R_a, back electromotive constant, K_b, motor torque constant K_m, motor moment of inertia, J_l. A saturation function is imbedded in the PID controller so that the voltage command to the DC motor would not exceed motor's physical limitations. The motor output is restricted by a dead zone dynamic function to accommodate friction loss; motor torque then converted to actuator force through a leadscrew.

The actuator force will be added to exciter force and two passive forces: spring force and damping force that drives the motion of the exercise platform. A sensor is used to feed platform displacement back to the PID controller that completes the loop.

The connecting structure between exercise platform and spacecraft structure is modeled as a passive control unit which includes a spring and a damper. Therefore, the force transmitted to the spacecraft equates the sum of spring force and damping force. When the motion of the platform is restricted, the transmitted force to the wall of spacecraft is also confined.

In this study, uncertainties and variations of system parameters are defined and included in the control loop. Controller gains and other system parameters are tuned under the consideration of the uncertainties and variations. A series of computer simulation for several ranges of uncertainties and variations was conducted. The results show excellent reduction of force being transmitted to the spacecraft structure while maintaining small platform displacement and acceleration.

II. Parameter Drift and Variation

"Drift" represents constants and parameters in a dynamic system that change their values over time. In the VIS, the main factor causing drift is the operating temperature. "Variation" stands for the change of input conditions. For example, exciter force changes from one exerciser to another exerciser on the exercise platform, or when a different exercise is being performed on the platform; even the same individual doing the same exercise could change intensity and frequencies over time.

A. Drift of Motor Constants

Motor parameters are considered to be "constants" when they are operated in an ideal situation. These constants will drift when the environment changes. The largest parameter drift in a DC motor is the armature resistance, R_a, as the function of temperature $R_a(f) = R_a(i) * \left[1 + \alpha_{conductor}\left(T_f - T_i\right)\right]$ [10]. As an example, $\boldsymbol{\alpha}$ for copper is 0.004.

S. B. Lin is with the Department of Mechanical Engineering at Prairie View A&M University, Prairie View, Texas 77446 USA (corresponding author, phone: 936-261-9958; e-mail: shlin@pvamu.edu).

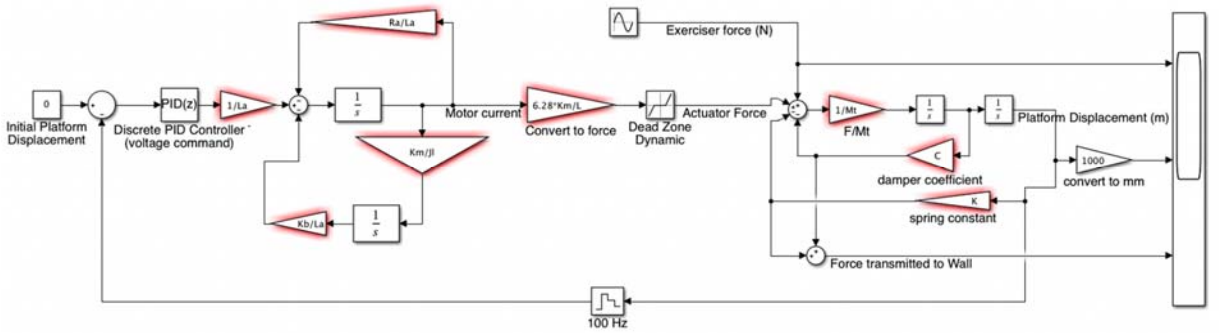

Fig. 1 Simulink Diagram of One-dimensional VIS for Astronaut's Exercise Platform [9]

Using the DC motor experimental data from a reference [11], the motor was operated at the initial temperature T_i = 24 °C and the final steady state temperature T_f = 60 °C. Applying the formula, the change of resistance is 0.004*(60-24) = 14.4%. If we select a nominal value of R_a at the average operating temperature, i.e., 42 °C, and assume a 10% variation of the resistance, we can obtain T_i and T_f.

- 10% = 0.004*(42 - T_i) results T_i = 17;
- 10% = 0.004*(T_f - 42) results T_f = 69.

This 10% variation allows the operating temperature to range from 17 °C to 69 °C, which covers a broader temperature range than the referenced DC motor experiment.

K_b, the back electromotive constant, and K_m, the motor torque constant, are directly related to magnetic flux density of the permanent magnets. In SI units, the value of K_m is equal to the value of K_b. The equation of these parameters with respect to temperature is very similar to the resistance equation [10].

$$K_b(f) = K_b(i) * \left[1 + \alpha_{magnet}\left(T_f - T_i\right)\right]$$

as an example: $\boldsymbol{\alpha}$ for Samarium Cobalt (SmCo) is -0.0004.

Since the coefficient of $\boldsymbol{\alpha}$ for Samarium Cobalt is one order lower than coefficient of $\boldsymbol{\alpha}$ for copper, 1% variation of K_b would be sufficient to match 10% variation of R_a in terms of operating temperature range.

Let us assume a 3% variation of K_b and K_m. By adding a couple of percentages in variation, it is possible to accommodate measurement error and material impurity.

L_a, the inductance of a DC motor is measured by applying a signal that is of sinusoidal form. It is then measured using the phase difference that is present between the voltage and current waveform. For accurate modeling results, the inductances must be measured under conditions approximating as closely as possible to those of normal operations [12]. Let us assume a 3% variation for measurement error of L_a.

B. Variation of Motor Inertia

The energy generated by electrical circuit and magnetic field in the DC motor will be converted to kinetic energy of mechanical motion and dissipation heat. The total kinetic energy, E_t, of the motor rotor is the sum of kinetic energy of the motor shaft with moment of inertia of the shaft, J_m, with angular velocity, ω, and the kinetic energy of the counterweight with mass, m, with linear velocity, v.

$$E_t = \frac{1}{2} J_m \omega^2 + \frac{1}{2} m v^2$$

The counterweight velocity can be represented by the lead screw pitch, L, and the motor angular velocity, ω, as $v = \frac{L}{2\pi}\omega$. We substitute this value in the kinetic energy equation yield:

$$E_t = \frac{1}{2}\left[J_m + m\left(\frac{L}{2\pi}\right)^2\right]\omega^2$$

Let $J_{eq} = \left[J_m + m\left(\frac{L}{2\pi}\right)^2\right]$ be the equivalent moment of inertia for the combined motor and counterweight at the motor shaft. Let's assume a 10% variation of the moment of inertia to accommodate both variations of the motor shaft and the load variation of the counterweight.

C. Uncertainty of Friction

Friction variation can be examined by the total energy loss to friction, E_f, which is the sum of energy loss at the motor shaft with friction coefficient, f_m, and angular velocity, ω, and the energy loss of the counterweight with friction coefficient, f_c, and linear velocity, v, which is equivalent to $\frac{L}{2\pi}\omega$.

$$E_f = \frac{1}{2}\left[f_m + f_c\left(\frac{L}{2\pi}\right)^2\right]\omega^2$$

The total mechanical torque consists of the kinetic motion via equivalent moment of inertia, J_{eq}, multiplies to angular acceleration, $\frac{d\omega(t)}{dt}$, and the torque lost to friction which is represented by the product of equivalent friction coefficient, f_{eq}, and angular velocity, $\omega(t)$. We equate mechanical torque to the torque generated by the electrical rotor circuit which is represented by the product of the motor constant, K_m, and the current, $i_a(t)$ which yields:

$$J_{eq}\frac{d\omega(t)}{dt} + f_{eq}\omega(t) = K_m i_a(t) \text{ where } f_{eq} = \left[f_m + f_c\left(\frac{L}{2\pi}\right)^2\right]$$

Friction coefficients can vary due to changes of temperature, surface cleanness, force level, etc. In this study, friction variation is treated as a "bounded" block, and is represented by a dead zone dynamic function for i_a which equates 0 when the input, u, is within a lower bound, lo, and an upper bound, up. When u is greater than up, it has an output of u-up; when u is

less than *lo*, it has an output of *u-lo*.

D. Variations in Passive Control Unit

The passive control unit can be represented by: $M_t\,\ddot{x} + c\,\dot{x} + k\,x = summation\ of\ forces$. The total mass, M_t, in the passive control equation is the sum of masses of the exerciser, the exercise platform, actuator components, and the counterweight. The major variation of M_t is the mass of exerciser.

In the beginning of the simulation, we wanted to keep the variation small, a 3% variation of M_t, and assume the VIS system is designed for a particular exerciser. As an imaginary real-scale system, an exerciser weights 200 lbs., the combination of exercise machine, exercise platform, linear actuator, and counterweight weights 200 lbs. A 3% variation of the total mass is +/- 12 lbs. That provides a weight range for the particular 200 lb exerciser from 188 lbs to 212 lbs, a good range to allow a person's weight fluctuation.

Spring constant k varies in a small amount when operating in its elastic range. Measurement of spring constant may carry some errors. We assume a 3% variation of the spring constant.

Damping coefficient c also varies in a small amount when operating environment is consistent. We assume a 3% variation for the damping coefficient.

E. Variations of Exciter Forces – Biking Exercise

Large variations of exerciser forces are anticipated on the VIS platform. Astronauts vary in height, weight, and body strength. Variations of types of exercise may send very different forces functions to the platform. Two types of force functions are used in our simulation runs:

(1) Sine wave function represents the biking exercise.
(2) Summation of step functions represents for pull-and-push exercise.

For the biking exercise, we selected a nominal force of 5 sin(5t) N for the 1D VIS prototype model; i.e., amplitude = 5N, and frequency = 5 rad/s. We assume that there is an amplitude variation of 200%; the largest force amplitude = 5 (1+200%) = 15 N.

Calculation of the smallest amplitude cannot be obtained by using the same nominal force as the base since the percentage is over 100%. An alternative approach by shifting the base to the smallest amplitude that gives the smallest amplitude = 5/(1+200%) = 1.7 N; we round off the value and use 2 N in the simulation.

We assume that there is a frequency variation of 400% in biking exercise; the largest force frequency = 5 (1+400%) = 25 rad/s. The same alternative approach is used to calculate the smallest force frequency = 5/(1+400%) = 1 rad/s.

During a biking exercise, amplitude and frequency changes are opposite to each other in general. When biking at low torque with high rotational speed, amplitude is generally low. When biking at high torque with low speed, the exerciser can move his/her body up and down with each rotational motion that can produce high amplitude for the exciter force.

F. Variations of Exciter Forces – Pull-and-Push Exercise

A "pull-and-push" exercise is somewhat similar to weight lifting on earth. Exciter force of pull-and-push exercise is generally affected by the accelerations of moving body parts of the exerciser and the machine components, and can be approximated to as a summation of a series of step functions.

In the simulation, the nominal force used in the 1D prototype model is represented by a 4-second cycle with force amplitudes within a boundary of +-10N. A 40% variation of force amplitude changes the boundaries of amplitude to +-6N at the low end to +-14N at the high end. An 80% variation of force cycle changes the exercise cycle from a 1-second cycle to 7-second cycle.

G. Summary of Variation Percentages

We performed a number of computer simulation runs based on the Simulink diagram of 1D VIS prototype shown in Fig. 1 with system parameters and the uncertainty percentages summarized as:

- Total mass M_t = 12 kg, with a variation of 3%,
- Spring constant k = 100 N/m, with a variation of 3%,
- Damping coefficient c = 10 N s/m, with a variation of 3%,
- Inductance of DC motor L_a = 0.003 H, with a variation of 3%
- Resistance of DC motor R_a = 3.0 Ω, with a variation of 10%,
- Back electromotive constant K_b = 0.105 V s/rad, variation: 3%,
- Motor torque constant K_m= 0.105 N m/A, variation: 3%,
- Motor moment of inertia J_l = 0.001 kg m^2, variation: 10%,
- Pull-and-push exercise force amplitude boundary F_0 = +-10 N, with a variation of 40%,
- Pull-and-push force cycle = 4 sec, with a variation of 80%,
- Biking exercise force amplitude F_0 = 5N, variation: 200%,
- Biking exercise force frequency ω = 5 rad/s, variation: 400%.

III. Simulation Results

A MATLAB script file is used to call a Simulink diagram, define system parameters and the percentages of variations of these system parameters. As shown in Fig. 2, the script file calls a Simulink file named 'Variations_sine,' defines system parameters, and uses a ureal() function to set percentages of uncertainty of each parameter. Force variations are supplied via input functions in the Simulink diagrams.

```
mdl = 'Variations_sine';
open_system(mdl)
%% Set nominal values
Mt=12.0;
k=100.0;
c=10.0;
La=0.003;
Ra=3.0;
Kb=0.105;
Km=0.105;
Jl=0.001;
%% Define uncertainty
Mt_un=ureal('Mt_un',Mt,'percentage',3);
k_un=ureal('k_un',k,'percentage',3);
c_un=ureal('c_un',c,'percentage',3);
La_un=ureal('La_un',La,'percentage',3);
Ra_un=ureal('Ra_un',Ra,'percentage',10);
Kb_un=ureal('Kb_un',Kb,'percentage',3);
Km_un=ureal('Km_un',Km,'percentage',3);
Jl_un=ureal('Jl_un',Jl,'percentage',10);
```

Fig. 2 MATLAB Script Defines Uncertainties

Control engineers widely use loop shaping method in the frequency domain to tune control systems to achieve desired behavior in terms of stability, performance, and robustness to model uncertainties and disturbances [13], [14]. In this study, loop shaping goal, gain margin and phase margin goal are defined in the tuning process for the VIS prototype model. The tuning algorithms calculate a sensitive function and a complementary sensitive function. These functions are formed by plant parameters and desired controller gains.

Minimizing the force transmitted to the wall, i.e., spacecraft structure, is the ultimate indicator of a well-tuned system. With the system parameter values and uncertainties that we used in the simulation, the tuning process returns a set of controller gains: P: 153.2, I = 567.9, D = 9.531, N = 1358; and "tuned" spring constant k = 66.41 and damping coefficient c = 10.36. Although these tuned values are obtained based on the defined variation percentages, the controller's robustness is actually beyond the defined parameter variations. These tuned controller gains and constants are used later for much larger parameter variations. Since the variations of exciter forces are not part of tuning process, a variety of exciter force functions is entered into the Simulink diagram for simulation runs. Three parameters, exciter force, platform displacement, and transmitted force, were chosen to be plotted via Simulink scope for comparison purpose.

As an example, we use the nominal force in biking exercise of 5 sin(5t) N as the exciter force, a Simulink output is shown in Fig. 3. The maximum transmitted force = 0.1487 N out of excited force of 5 N, a 97.03% force reduction with reasonably small platform displacement = 1.385 mm.

Another example uses larger force amplitude and smaller frequency exciter force 15 sin(t). As shown in Fig. 4, Simulink output a maximum transmitted force = 0.1752 N out of excited force of 15 N, a 98.83% force reduction while maintaining small platform displacement = 2.611 mm.

Fig. 3 Output of Biking Exciter Force 5sin(5t) N

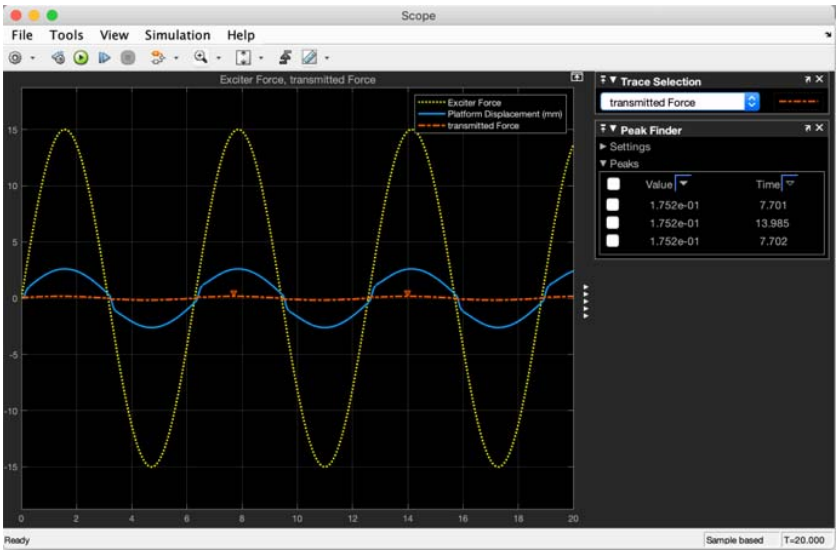

Fig. 4 Output of Biking Exciter Force 15sin(t) N

A number of simulations is run and recorded between exciter force frequencies of 1 rad/s and 25 rad/s as defined for biking exercise. The results of percentage of force reduction versus exciter force frequencies are plotted in Fig. 5 which indicates the lowest percentage of force reduction taking place at the exciter force frequency of 16 rad/s.

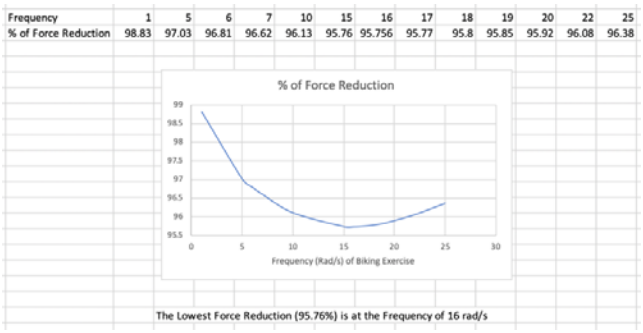

Fig. 5 Percentage of Force Reduction vs. Frequency

For a pull-and-push exercise, simulation runs were performed using the same controller gains and passive control constants as in the biking exercise. Many simulation runs are performed using different combinations of step functions as the exciter force. The force reduction percentages of transmitted force to wall versus the exciter force are comparable to those in the biking exercises. As an example of pull-and-push exercise simulation shown in Fig. 6, the exciter force is represented by a combination of step functions with amplitudes within boundaries of +-8 N and pull-and-push cycle of 2 seconds. Simulation results show the maximum transmitted force to wall = 0.2151 N, a 97.31% force reduction from the exciter force.

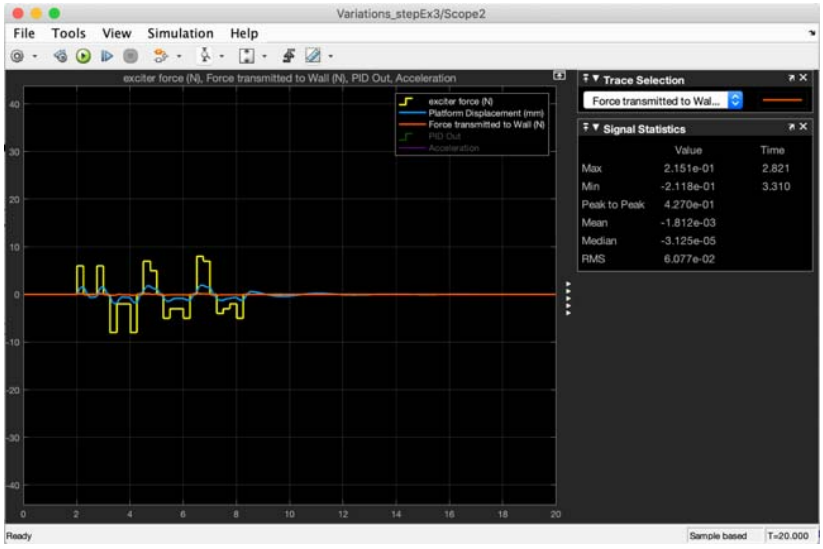

Fig. 6 Output of pull-and-push exciter forces

A. Trick vs. Simulink

Trick Simulation Toolkit is a simulation program in C/C++ and Java. It was developed at NASA Johnson Space Center with the assistance of L-3 Communications and CACI Companies. Many high-fidelity training programs and engineering simulations at the NASA Johnson Space Center and other NASA facilities use Trick as a main development tool [15]. It provides automated job scheduling, data recording, interactive variable manipulation, and many other capabilities. As part of the task, we develop the same active-controlled vibration isolation model as shown in Fig. 1 using C/C++, and run the simulation through Trick. The initial purpose is to compare the simulation results between a commercial simulation tool, MATLAB/Simulink, and the NASA simulation Toolkit, Trick.

We used Simulink to run the diagram model and plotted output for five parameters, including exciter force, platform displacement, force transmitted to wall, PID command, and platform acceleration as shown in Fig. 7.

We also used Trick to run C/C++ model. The same five parameters were plotted as shown in Fig. 8. The graph looks identical as the one obtained in Simulink. Simulation results in terms of values between the two simulations are almost identical. As shown in Fig. 9, platform displacement (Disp) has four precision points in Simulink and 6 precision points in Trick, the difference is only happened at the two extra insignificant decimal points obtained in Trick simulation. If we round up the result in Trick to match four precision points in Simulink, the two values would be identical.

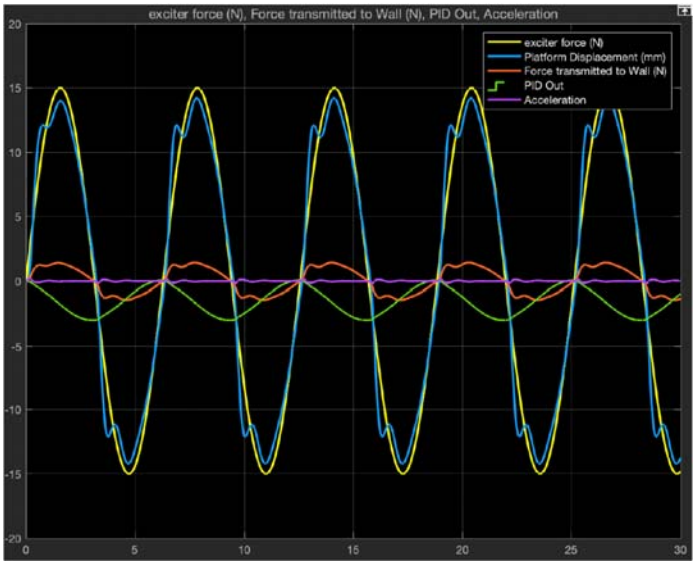

Fig. 7 Output of 5 parameters in Simulink

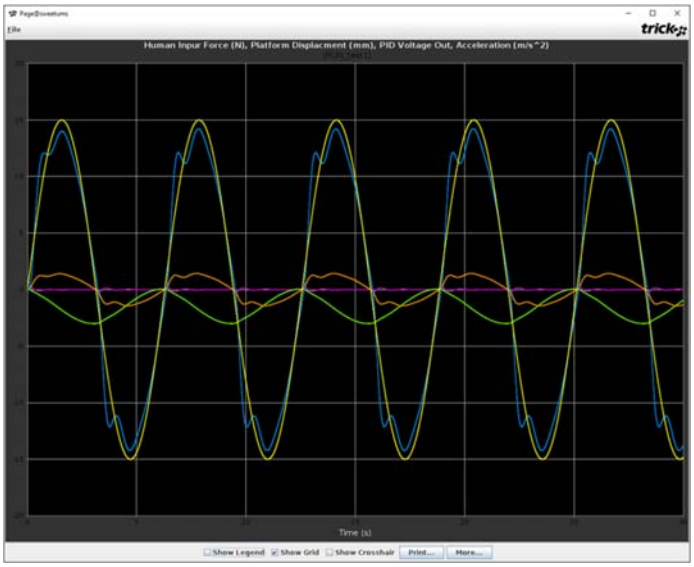

Fig. 8 Output of 5 parameters in Trick

Disp	Time	Simulink	Trick	Difference
MAX	14.109	14.22 mm	14.2205 mm	~ 0.0005 mm
MIN	4.684	-14.22 mm	-14.2223 mm	~ 0.0023 mm

Fig. 9 Platform Displacement in Simulink and Trick

Another example is shown in Fig. 10, force transmitted to wall (F_wall) has four precision points in Simulink and five precision points in Trick, the difference is only apparent with the extra insignificant decimal point obtained in Trick simulation. If we round up the result in Trick to match four precision points in Simulink, the two values would be identical.

F_wall	Time	Simulink	Trick	Difference
MAX	26.576	1.438 N	1.4384 N	~ 0.0004 N
MIN	4.584	-1.439 N	-1.4385 N	~ 0.0005 N

Fig. 10 Force Transmitted to Wall in Simulink and Trick

B. Monte Carlo Simulation for Larger Variations

Monte Carlo is an advanced simulation capability provided by Trick that allows users to repeated run copies of a simulation with different input values [16]. This feature provides a convenient means to set ranges of simulation parameters for uncertainties and variations in the VIS system.

We initially apply Monte Carlo tool in Trick to simulate the parameter variations based on the percentages of parameter drift and variations discussed earlier in this paper. In 1,000 simulation runs of randomly selected parameter values within the defined ranges, key output variables of the system are recorded in the simulation results. It is evident that both platform displacement and transmitted force remain small within the defined variations of system parameters. We then push the variation boundaries to run the Monte Carlo simulation within larger parameter variations. After several pushes of the

variation boundaries, we stopped at quite large ranges of parameter variations as summarized in the following:

- Total mass M_t = 12 kg, with a variation of 50%,
- Spring constant k = 66.41 N/m, with a variation of 20%,
- Damping coefficient c = 10.36 N s/m, with a variation of 20%,
- Inductance of DC motor L_a = 0.003 H, with a variation of 20%
- Resistance of DC motor R_a = 3.0 Ω, with a variation of 20%,
- Back electromotive constant K_b = 0.105 V s/rad, variation 20%,
- Motor torque constant K_m= 0.105 N m/A, variation 20%,
- Motor moment of inertia J_l = 0.001 kg m^2, variation 20%.

The significant variation of 50% for the total mass M_t in the prototype allows its value swing between 6 kg to 18 kg. For an equivalent real-scale system ignoring the masses of platform and other devices, we assume an exerciser with a nominal mass of 200 lbs, the 50% variation would allow the exerciser mass changing from 100 lbs to 300 lbs. This variation would cover very wide ranges of body masses for entire crew members who might use the exercise platform. The 20% variations for seven system parameters provide safe buffers for material impurity, manufacturing defect, temperature variation, and other damaging factors that might cause parameters changes.

Fig. 11 displays the "worst scenario" of the Monte Carlo results. The simulation was run under the exciter force frequency of 16 rad/s which gives the lowest percentage of force reduction as shown earlier in Fig. 5. With the wide variation of 50% for M_t, and 20% for the remaining parameters, the worst transmitted force equal to -0.272692413N at run #676 in a one-thousand runs. The percentage of force reduction is 94.55% from the exciter force of 5sin(16t) N. The largest platform displacement under this particular case is -1.269 mm for the prototype model. Small movement and acceleration provide reasonable comfortability to the users of the exercise platform.

RUN #	Max Force (N)	Time	Min Force (N)	Time	Max POS (mm)	Time	Min POS (mm)	Time
676	0.264682647	0.528	-0.272692413	0.325	1.231535449	0.192	-1.268548079	0.406
446	0.264665968	0.528	-0.272672164	0.325	1.231500087	0.192	-1.268523053	0.406
277	0.264442549	0.527	-0.272387522	0.325	1.23100365	0.192	-1.268168184	0.406
977	0.264347931	0.527	-0.272266701	0.325	1.230795026	0.191	-1.268015878	0.406
452	0.264248479	0.527	-0.272140338	0.325	1.23058387	0.191	-1.267855551	0.406
366	0.264179336	0.527	-0.272052833	0.325	1.230437737	0.191	-1.267743921	0.406
535	0.264152883	0.527	-0.272019425	0.325	1.230381951	0.191	-1.26770117	0.406
327	0.264120745	0.527	-0.271978888	0.325	1.230314262	0.191	-1.2676492	0.406

Fig. 11 "Worst Scenario" in Monte Carlo Simulation

IV. Conclusions

Uncertainties of system parameters such as motor constants, damping coefficient, mass, etc. are defined and built in the one-dimensional active-controlled VIS prototype model for astronaut's exercise platform. Variations of exciter force are also defined for biking and pull-and-push exercises. Robust control tuning processes in Simulink are applied to tune the controller gains via Loop Shape method and Gain/Phase Margins method. The tuning process is also used to obtain a desirable spring constant and damping coefficient of the passive unit.

Simulation was performed using MATLAB/Simulink with the tuned controller gains, spring constant, and damping coefficient. High percentage of force reduction (more than 95%) were shown in all runs under biking exercise frequencies ranging from 1 rad/s to 25 rad/s as well as a variety of combinations of step functions for pull-and-push exercise.

Trick is applied as another simulation tool to compare its simulation results to that in Simulink. The results show almost identical graphs and data values obtained in both simulation programs. The Monte Carlo tool in Trick is applied to push the boundaries of system parameter variations. Excellent force reduction (near 95%) is obtained for the VIS under very wide variations of system parameters and exciter forces.

Acknowledgment

The authors would like to thank Robert Zehentner, Daniel Erdberg, and Fouad Matari of CACI, Leslie Quiocho and Mike Red at NASA Johnson Space Center (JSC), and many other colleagues working at JSC for the research opportunities, sponsorship and support. This material does not contain controlled technical data as defined within the International Traffic in Arms (ITAR) Part 120.10 or Export Administration Regulations (EAR) Parts 772 and 774. (Approved 01/22/2021)

References

[1] J.R. Bagley, K.A. Murach, and S.W. Trappe, "Microgravity-Induced Fiber Type Shift in Human Skeletal Muscle." Gravitational and Space Biology, Volume 26(1), pp. 34-40, April 2012.

[2] A. Hawkey, "The Importance of Exercising in Space," Interdisciplinary Science Reviews, 28:2, 130-138, 2003.

[3] A.J. Calise, J.I. Craig, and B-J Yang, "Adaptive Control for a Microgravity Vibration Isolation System," Finial report, NASA Marshall Space Flight Center, Huntsville, AL, March 2006.

[4] C. Grodsinsky and G. Brown, "Nonintrusive Inertial Vibration Isolation Technology for Microgravity Space Experiments," Aerospace Research Central, AIAA-90-0741, August 2012.

[5] V.C. Nguyen, "A Method to Determine the Optimal Parameters for PID Controller," International Journal of Engineering and Applied Sciences, Volume-6, Issue-1, January 2019.

[6] M. Pabst, M. Darnieder, and R. Theska, "Measuring and Adjusting the Stiffness and Tilt Sensitivity of a Novel 2D Monolithic High Precision Electromagnetic Force Compensated Weighing Cell," NCSL International Workshop & Symposium, Cleveland, Ohio, August 2019.

[7] A.C. Ihedioha and A.M. Anyanwu, "Implementation of an Elevator's Position-Controlled Electric Drive," International Journal of Trend in Research and Development, Volume 3(5), September 2016.

[8] K. Karaman, Y.T. Bekaroglu, M.T. Soylemez, K. Ucak, and G.O. Gunel, "Controlling 3-DOF Helicopter via Fuzzy PID Controller," International Conference on Electrical and Electronics Engineering, Bursa, Turkey, November 2015.

[9] S.B. Lin and S. Abdali, "Simulation of Active Controlled Vibration Isolation System for Astronaut's Exercise Platform," International Journal of Mechanical and Mechatronics Engineering, Vol. 15, No.2, pp.107-112, 2021.

[10] D. Montone, "Understanding DC Motor Curves and Temperature," PITTMAN Motors/AMETEK Precision Motion Control, November 2013.

[11] I. Garniwa, et al, "Analysis of the Effect of the Motor Temperature to Brushless Direct Current Motor Performance on KARLING Electric Vehicle," 2019 Journal of Physics: Conference Series 1376 012024.

[12] N. Chuang, T. Gale, R. Langman, "Measuring Inductances on a DC Motor," School of Engineering, University of Tasmania, Hobart, Tasmania, Australia.

[13] D. Bruijnen, R. van de Molengraft, and M. Steinbuch, "Optimization Aided Loop Shaping for Motion Systems,"2006 IEEE Conference on Computer Aided Control System Design.

[14] "Control Systems – Loopshaping" MIT Open Course Ware, http://ocw.mit.edu, 2.017J Design of Electromechanical Robotic Systems Fall 2009.
[15] J.M. Penn and A.S. Lin, "The Trick Simulation Toolkit: A NASA/Open source Framework for Running Time Based Physics Models," AIAA SciTech Forum, January 1, 2016.
[16] S. Fennell, "Monte Carlo Tutorial," GitHub pages public repositories website, May 16, 2019.